Enhancement of the Dimensionality of Molecular π Conductors by the Selone Substitution of M(dmit)$_2$ (M = Ni, Pd) Systems: Newly Synthesized dmise Compounds [Me$_x$H$_{4-x}$N][Ni(dmise)$_2$]$_2$ (x = 1−3) and Cs[Pd(dmise)$_2$]$_2$ (dmise = 4,5-Dimercapto-1,3-dithiole-2-selone)

Akane Sato,[†] Hayao Kobayashi,[†] Toshio Naito,[‡] Fumiko Sakai,[§] and Akiko Kobayashi*[,||]

Department of Functional Molecular Science, School of Mathematical and Physical Science, The Graduate University for Advanced Studies and Institute for Molecular Science, Okazaki 444, Japan, Department of Chemistry, Faculty of Science, Hokkaido University, Sapporo, Hokkaido 060, Japan, Institute for Solid State Physics, The University of Tokyo, Roppongi, Minato-ku, Tokyo 106, Japan, and Department of Chemistry, School of Science, The University of Tokyo, Hongo, Bunkyo-ku, Tokyo 113, Japan

Received May 1, 1997[⊗]

Single crystals of [Me$_3$HN][Ni(dmise)$_2$]$_2$, [Me$_2$H$_2$N][Ni(dmise)$_2$]$_2$, [MeH$_3$N][Ni(dmise)$_2$]$_2$, and Cs[Pd(dmise)$_2$]$_2$ were grown electrochemically. The crystal structures of [Me$_3$HN][Ni(dmise)$_2$]$_2$, [Me$_2$H$_2$N][Ni(dmise)$_2$]$_2$, and [MeH$_3$N][Ni(dmise)$_2$]$_2$ were determined. Crystal data are as follows: [Me$_3$HN][Ni(dmise)$_2$]$_2$ ($C_{15}H_{10}NNi_2S_{16}Se_4$), triclinic, $P\bar{1}$, a = 7.606(3) Å, b = 17.761(3) Å, c = 6.660(2) Å, α = 100.27(2)°, β = 114.93(2)°, γ = 81.84(2)°, Z = 1; [Me$_2$H$_2$N][Ni(dmise)$_2$]$_2$ ($C_{14}H_8NNi_2S_{16}Se_4$), triclinic, $P\bar{1}$, a = 7.625(3) Å, b = 17.583(5) Å, c = 6.526(2) Å, α = 100.01(2)°, β = 114.81(5)°, γ = 80.82(5)°, Z = 1; [MeH$_3$N][Ni(dmise)$_2$]$_2$ ($C_{13}H_6NNi_2S_{16}Se_4$), monoclinic, $P2_1/c$, a = 7.636(2) Å, b = 9.545(3) Å, c = 22.555(6) Å, β = 92.95(2)°, Z = 2. Short contacts between Se atoms across the cation sheet were found in [Me$_3$HN][Ni(dmise)$_2$]$_2$ and [Me$_2$H$_2$N][Ni(dmise)$_2$]$_2$. A tight-binding band structure calculation by extended Hückel methods indicated that [Me$_3$HN][Ni(dmise)$_2$]$_2$ has even stronger intermolecular interactions along the long molecular axis than along the transverse direction owing to a close selenium−selenium contact. Cs[Pd(dmise)$_2$]$_2$ kept metallic behavior down to 4 K at ambient pressure.

Introduction

The Ni(dmit)$_2$ complex molecule (dmit = 4,5-dimercapto-1,3-dithiole-2-thione) has played an important role in the development of new molecular conducting systems, from which the first molecular superconductor based on transition-metal-complex molecules has been prepared.[1,2] Unlike most of the constituent molecules of crystalline molecular conductors, which are TTF-like π-donor molecules, Ni(dmit)$_2$ is a π-acceptor molecule. Despite the resemblance in the molecular structures and the modes of molecular arrangements between Ni(dmit)$_2$ and BEDT-TTF (=bis(ethylenedithio)tetrathiafulvalene), it has been pointed out that the transverse intermolecular interactions in the Ni(dmit)$_2$ conductors are not so strong owing to the nodal plane of the lowest unoccupied molecular orbital (LUMO) on the central Ni atom, from which the conduction bands are formed.[3] In the cases of the Pd(dmit)$_2$ conductors with strongly dimerized stacking structures, the highest occupied molecular orbitals are mainly responsible for the electronic band formation, but their metallic nature tends to be weak because of the existence of the large mid-gaps, which makes the effective band width narrow. Nevertheless, various types of molecular conductors including some stable metallic systems and seven molecular superconductors have been discovered in M(dmit)$_2$ (M = Ni, Pd) salts.

Compared with the TTF-like π-donor molecules, M(dmit)$_2$ molecules have the unique advantage that they can interact with each other through the terminal thione groups of dmit ligands along the direction of the long axis of the molecule. Such a possibility was suggested 10 years ago in [Et$_4$N][Ni(dmit)$_2$]$_2$, which was regarded as a precursor of a three-dimensional molecular metal in spite of its semiconducting properties.[4] Until now, there has been no example of a single-crystal molecular metal whose three-dimensional Fermi surface was determined by low-temperature physical experiments such as Shbnikov−de Haas and/or de Haas−van Alphen experiments. Of course, the design of three-dimensional molecular metals based on planar π molecules will be not so easy, but the development of such a system may be one of the important future targets of the chemistry of molecular conductors.

M(dmise)$_2$ (dmise = 4,5-dimercapto-1,3-dithiole-2-selone) is a π-acceptor molecule analogous to M(dmit)$_2$, where thione groups are replaced by selone groups. It may be easily imagined that the three-dimensionality will be enhanced greatly by replacing the thione group with a selone group, if we can obtain M(dmise)$_2$ conductors with structures similar to those of the corresponding M(dmit)$_2$ conductors.

The crystal structures and physical properties of the first partially oxidized M(dmise)$_2$ salts, α- and β-[Me$_4$N][Ni-

[†] The Graduate University for Advanced Studies and Institute for Molecular Science.
[‡] Hokkaido University.
[§] Institute for Solid State Physics.
[||] The University of Tokyo.
[⊗] Abstract published in *Advance ACS Abstracts,* October 1, 1997.

(1) Cassoux, P.; Valade, L.; Kobayashi, H.; Kobayashi, A.; Clark R. A.; Underhill, A. E. *Coord. Chem. Rev.* **1991**, *110*, 115.
(2) Brossard, L.; Ribault, M.; Valade, L.; Cassoux, P. *Physica B+C (Amsterdam)* **1986**, *143*, 378.
(3) Kobayashi, A.; Kobayashi, H. in Molecular Metals and Superconductors Based on Transition Metal Complexes. In *Handbook of Organic Conductive Molecules and Polymers*; Nalwa, N., Ed.; John Wiley & Sons: New York, 1997; Chapter 5.
(4) Kato, R.; Mori, T.; Kobayashi, A.; Sasaki, Y.;. Kobayashi, H. *Chem. Lett.* **1988**, 865.

S0020-1669(97)00507-7 CCC: $14.00 © 1997 American Chemical Society

Scheme 1

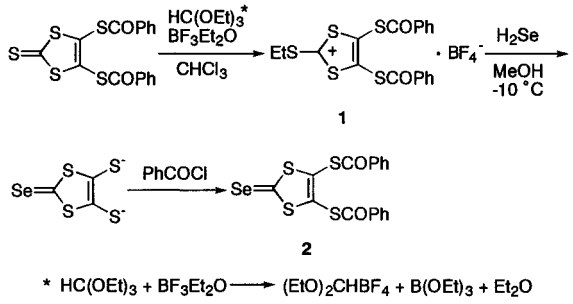

$(dmise)_2]_2$, were reported by Cornelissen et al.[5,6] Although the room-temperature conductivity was as high as that of BEDT-TTF salts ($\sim$10 S cm^{-1}), the systems behaved as semiconductors. The most prominent feature in the crystal structure of α-$[Me_4N][Ni(dmise)_2]_2$ is the extremely short intermolecular Se$\cdots$Se contact between terminal selone groups, which is more than 0.72 Å shorter than the sum of the van der Waals radii (i.e., 4 Å). However, the calculation of the intermolecular overlap integrals of LUMOs showed the selone−selone interaction to be very small, and both α- and β-$[Me_4N][Ni(dmise)_2]_2$ systems were suggested to have quasi-one-dimensional band structures. These results indicated the difficulty in the design of three-dimensional molecular metals from usual planar π molecules. But the small interaction between the selone groups is not an unexpected result because of the large sensitivity of the $\pi-\pi$ overlap integrals to the mutual orbital orientations.

Most of the molecular conductors currently studied have layered structures, where the neighboring conduction layers constituted of planar π molecules are separated by counterions between them. Since the layer−layer separation depends on the size of the counterions, smaller size anions would be preferable to obtain conductors with large interlayer interactions. In this study we examine the possibility of enhancing three-dimensional interaction by synthesizing new $M(dmise)_2$ conductors with small anions. Such are $[Me_xH_{4-x}N][Ni(dmise)_2]_2$ (x = 1−3) and $Cs[Pd(dmise)_2]_2$.

Experimental Section

Synthesis of Ligands. The synthesis of the dmise ligand has been described in the literature.[5−10] We adopted the synthetic route reported by Cornelissen et al.[6] But a slight modification has been made in order to improve the reproducibility of the synthesis (Scheme 1). All of the reactions were carried out under a nitrogen atmosphere, and solvents were distilled before use.

2-(Ethylthio)-4,5-bis(benzoylthio)-1,3-dithiolium Tetrafluoroborate, 1. Triethyl orthoformate (3.9 g, 25 mmol) and boron trifluoride diethyl ether complex (10.5 g, 34 mmol) were added successively to a chloroform solution (70 mL) of $(dmit)(COPh)_2$ (6.1 g, 15 mmol). The solution was refluxed for 3.5 h and cooled in an ice bath. Dried diethyl ether (180 mL) was added, and the red tarry precipitate was filtered off. The red solid changed to pale yellow powder after air-drying. The product **1** was used without further purification (7.4 g, 92%): ν_{max}/cm^{-1} 1376 m (S−C), 1207 m (C═S), 1051 (BF_4^-), 1461, 684 (Ph), 1677 (COPh); m/z 406 (M − Et), 362 (M − EtSC), 330 (M − EtSCS), 105 (COPh).

Table 1. Summary of Crystal Data and Intensity Measurements for $[Me_3HN][Ni(dmise)_2]_2$ (**a**), $[Me_2H_2N][Ni(dmise)_2]_2$ (**b**), and $[MeH_3N][Ni(dmise)_2]_2$ (**c**)

	a	**b**	**c**
empirical formula	$C_{15}H_{10}NNi_2S_{16}Se_4$	$C_{14}H_8NNi_2S_{16}Se_4$	$C_{13}H_6NNi_2S_{16}Se_4$
cryst syst	triclinic	triclinic	monoclinic
space group (No.)	$P\bar{1}$ (No. 2)	$P\bar{1}$ (No. 2)	$P2_1/c$ (No. 14)
a (Å)	7.606(3)	7.625(3)	7.636(2)
b (Å)	17.761(3)	17.583(5)	9.545(3)
c (Å)	6.660(2)	6.526(2)	22.555(6)
α (deg)	100.27(2)	100.01(2)	
β (deg)	114.93(2)	114.81(5)	92.95(2)
γ (deg)	81.84(2)	80.82(5)	
V (Å^3)	800.4(4)	778.4(4)	1641.6(8)
Z	1	1	2
λ(Mo Kα) (Å)	0.7107	0.7107	0.7107
ρ_{calc} (g cm^{-3})	2.387	2.425	2.267
μ(cm^{-1})	67.84	69.74	66.0
T (K)	296	296	296
R (F_o)[b]	0.036	0.066	0.058
R_w (F_o)	0.022[c]	0.072[d]	0.058[c]

[a] $|F_o| \geq 3\sigma|F_o|$. [b] $R = \sum(|F_o| - |F_c|)/\sum|F_o|$. [c] $R_w = \sum w(|F_o| - |F_c|)^2$, $w = 1/\sigma^2(F)$. [d] $R = [\sum w(|F_o - |F_c|)^2/\sum w|F_o|^2]^{1/2}$, $w = 1/\sigma^2(F)$.

Table 2. The Exponents ζ and the Ionization Potentials (eV) for Atomic Orbitals

orbital	ζ	E_i (eV)
Se		
4s	2.112	−20.0
4p	1.827	−11.0
4d	1.5	−6.8
S		
3s	2.122	−20.0
3p	1.825	−11.0
3d	1.5	−5.44
Ni		
4s	2.1	−7.34
4p	2.1	−3.74
4d	*a*	−10.6
C		
2s	1.625	−21.4
2p	1.625	−11.4

[a] Double ζ: $0.5681\chi_1$ (5.75) + $0.6294\chi_2$ (2.0).

4,5-Bis(benzoylthio)-1,3-dithiole-2-selone, 2. Small portions of solid **1** (7.4 g, 14.1 mmol) were added at 0 °C to a methanol solution of H_2Se,[6] which was prepared *in situ* from elemental selenium (3.2 g, 41 mmol) and sodium tetrahydroborate in methanol (100 mL) and acetic acid (4 mL). The resulting solution was stirred for 3.5 h at 0 °C and then 30 min at room temperature. Benzyl chloride (29 mL) was added to the reddish-purple solution, and reddish-orange needle crystals of **2** were precipitated. $(dmise)(COPh)_2$ was isolated by dichloromethane/hexane (1:1)/silica gel column chromatography and recrystallized from dichloromethane/methanol (4.1 g, 64%): ν_{max}/cm^{-1} 1682 s (C═O), 958 (C═Se), 881s (C−S), 1446 w, 1205 s, 348 s (Ph); m/z 454 (M^+), 105 (COPh), 77 (Ph). Found: C, 44.77; H, 2.35; S, 27.92, Se, 16.91. $C_{17}H_{10}S_4SeO_2$ requires C, 45.03; H, 2.22; S, 28.92; Se, 16.91).

$[n$-Bu$_4$N$]_2$[M(dmise)$_2$] (M = Ni and Pd), 3, and $[n$-Bu$_4$N][Ni(dmise)$_2$], 4. The compounds were prepared in analogy to the synthesis of the dmit complexes as described by Steimecke et al.[11]

Preparation of Charge-Transfer Complexes. Single crystals of $[Me_3HN][Ni(dmise)_2]_2$, $[Me_2H_2N][Ni(dmise)_2]_2$, and $[MeH_3N][Ni(dmise)_2]_2$ were obtained by electrochemical oxidation of a mixture of $[Bu_4N][Ni(dmise)_2]$ (4−6 mg) and the proper supporting electrolyte as the ClO_4 salts (80−135 mg) in acetonitrile or a mixed solution of acetone and acetonitrile (1:1, v/v; 15 mL). A constant current of 0.2 μA was applied at 10 or 20 °C for 4−7 days. In most cases, the products were obtained as very thin and small plate crystals. $[Me_3HN][Ni(dmise)_2]_2$ and $[Me_2H_2N][Ni(dmise)_2]_2$ were unstable in air. Crystals

(5) Cornelissen, J. P.; Reefman, D.; Haasnoot, G.; Spek, A. L.; Reedijik, J. *Recl Trav. Chim. Pays-Bas* **1991**, *110*, 345.
(6) Cornelissen, J. P.; Pomarde, B;. Spek, A. L.; Reefman, D.; Haasnoot, J. G.; Reedijk, J. *Inorg. Chem.* **1993**, *32*, 3720.
(7) Khodorkozskii, V. Y.; Kreicberga, J.; Balodis, K. A.; Neiland, O. Y. *Izv. Akad. Nauk Latv. SSR, Ser. Khim.* **1988**, 120.
(8) Kobayashi, H.; Kato, R;. Kobayashi, A. *Synth. Met.* **1991**, *42*, 2495.
(9) Olk, B.; Olk, R.-M.; Sieler, J.; Hoyer, E. *Synth. Met.* **1991**, *42*, 2585.
(10) Naito, T.; Sato, A.; Kawano, K.; Tateno, A.; Kobayashi, H.; Kobayashi, A. *J. Chem. Soc., Chem. Commun.* **1995**, 351.
(11) Steimecke, G.; Sieler, H. -J.; Kirmse R.; Hoyer, E. *Phosphorus Sulfur Relat. Elem.* **1979**, *7*, 49.

Table 3. Atomic Coordinates of $[Me_3HN][Ni(dmise)_2]_2$ and $[Me_2H_2N][Ni(dmise)_2]_2$

atom	*x*	*y*	*z*	B_{eq}[a]
		(a) $[Me_3HN][Ni(dmise)_2]_2$		
Se1	0.1765(1)	0.13814(4)	0.0814(1)	4.60(2)
Se2	0.3974(1)	0.93242(4)	0.0699(1)	4.57(2)
Ni	0.2638(1)	0.53380(4)	0.0334(1)	2.45(1)
S1	0.2716(2)	0.47219(8)	0.2878(2)	3.01(3)
S2	0.1991(2)	0.43341(8)	−0.2168(2)	3.06(3)
S3	0.2294(2)	0.30646(8)	0.2844(2)	3.15(4)
S4	0.1620(2)	0.26925(8)	−0.1801(2)	3.33(4)
S5	0.3311(2)	0.63056(8)	0.2926(2)	3.02(3)
S6	0.2509(2)	0.59925(8)	−0.2185(2)	2.91(3)
S7	0.3842(2)	0.79435(8)	0.2833(2)	3.18(4)
S8	0.3085(2)	0.76748(8)	−0.1825(2)	3.25(4)
N	0.910(1)	0.9832(5)	0.455(2)	15.0(4)
C1	0.233(7)	0.3822(3)	0.1533(8)	2.4(1)
C2	0.2008(7)	0.3652(3)	−0.0678(8)	2.6(1)
C3	0.1877(7)	0.2362(3)	0.0609(8)	2.9(1)
C4	0.3357(7)	0.7015(3)	0.1550(8)	2.4(1)
C5	0.3019(7)	0.6880(3)	−0.0675(8)	2.5(1)
C6	0.3637(7)	0.8342(3)	0.0574(8)	2.9(1)
C7	0.964(2)	0.9113(8)	0.522(2)	20.4(6)
C8	1.198(2)	0.9627(10)	0.465(2)	18.6(5)
		(b) $[Me_2H_2N][Ni(dmise)_2]_2$		
Se1	0.8767(3)	0.9372(1)	0.7585(3)	3.73
Se2	0.6707(3)	0.1373(1)	−0.2513(3)	3.65
Ni	0.7631(3)	0.5335(1)	0.2713(3)	1.98
S1	0.7476(6)	0.6006(2)	0.5779(6)	2.45
S2	0.8281(6)	0.6342(5)	0.1687(5)	2.46
S3	0.4002(6)	0.4340(2)	0.3668(6)	2.64
S4	0.7299(6)	0.3064(2)	−0.2387(6)	2.58
S5	0.8736(6)	0.7999(2)	0.3898(6)	2.78
S6	0.7732(6)	0.4732(2)	−0.0391(6)	2.50
S7	0.7982(6)	0.7699(2)	0.7644(6)	2.84
S8	0.6628(6)	0.2687(2)	0.1340(6)	2.84
N	0.522(8)	−0.025(2)	−0.005(8)	8.43
C1	0.847(2)	0.8379(8)	0.638(2)	2.52
C2	0.685(2)	0.2363(8)	−0.122(2)	2.57
C3	0.700(2)	0.3645(7)	0.150(2)	2.14
C4	0.733(2)	0.3822(7)	−0.028(2)	2.29
C5	0.793(2)	0.6909(8)	0.562(2)	2.35
C6	0.832(2)	0.7046(7)	0.385(2)	2.43
C11	0.376(5)	−0.004(2)	−0.171(4)	4.31
C12	0.623(5)	0.050(3)	0.231(5)	5.31

[a] $B_{eq} = (8/3)\pi^2(U_{11}(aa^*)^2 + U_{22}(bb^*)^2 + U_{33}(cc^*)^2 + 2U_{12}aa^*bb^* \cos\gamma + 2U_{13}aa^*cc^* \cos\beta + 2U_{23}cc^*bb^* \cos\alpha)$.

of $Cs[Pd(dmise)_2]_2$ were obtained by electrochemical oxidation of mixture of $[Bu_4N]_2[Pd(dmise)_2]$ (8 mg) and $CsPF_6$ (160 mg) in a mixed solution of acetone and acetonitrile (15 mL). A constant current of 0.8 μA was applied at 20 °C for 10 days. The products were obtained as very thin and warped crystalline solids.

X-ray Crystal Structure Determination. $[Me_3HN][Ni(dmise)_2]_2$. Intensity data were collected at 23 °C on an automatic four-circle diffractometer (Rigaku AFC-5R) equipped with a rotating anode. Monochromated Mo Kα radiation was used. The empirical absorption corrections were made. The crystal data are listed in Table 1. The structure was solved by direct methods. Anisotropic temperature factors were used for the non-hydrogen atoms and refined by full-matrix least-squares methods. The hydrogen atoms were included in the final calculation. The atomic scattering factors were taken from ref 12. All calculations were performed using the teXsan crystallographic software package of Molecular Structure Corporation.[13]

$[Me_2H_2N][Ni(dmise)_2]_2$. Intensity data were collected at 23 °C on an automatic four-circle diffractometer (Rigaku AFC-7R) with Mo Kα radiation. Empirical absorption corrections were made. The crystal data are listed in Table 1. The structure was solved by heavy-atom methods. Anisotropic temperature factors were used for the non-hydrogen atoms and refined by block-diagonal least-squares methods. The hydrogen atoms were not included in the final calculation. All of the calculations were performed on a HITAC M-680 computer at the Computer Center of the University of Tokyo using the program UNICS III.[14]

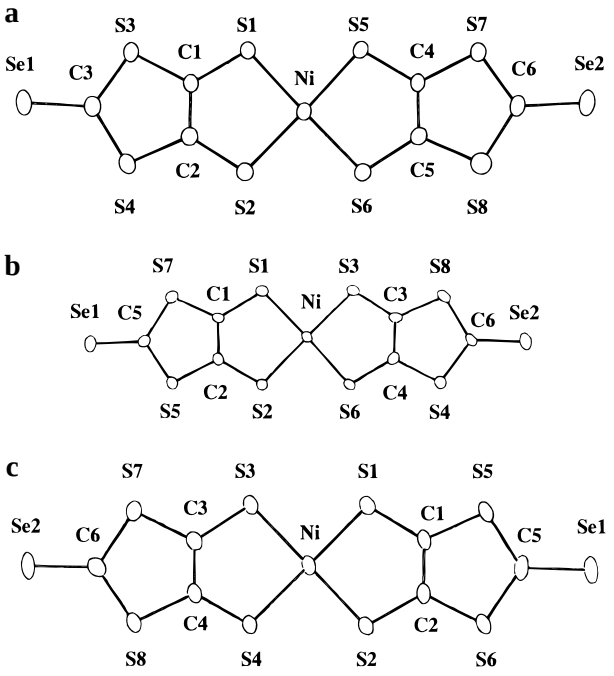

Figure 1. Perspective views of $Ni(dmise)_2$ of (a) $[Me_3HN][Ni(dmise)_2]_2$, (b) $[Me_2H_2N][Ni(dmise)_2]_2$, and (c) $[MeH_3N][Ni(dmise)_2]_2$. Thermal ellipsoids are at the 30% probability level.

$[MeH_3N][Ni(dmise)_2]_2$. Intensity data were collected at 23 °C on an automatic four-circle diffractometer (Rigaku AFC-7R) with Mo Kα radiation. Empirical absorption corrections were made. The crystal data are listed in Table 1. The structure was solved by direct methods. Anisotropic temperature factors were used for the non-hydrogen atoms and refined by full-matrix least-squares methods. The hydrogen atoms were not included in the final calculation. All of the calculations were performed using the teXsan crystallographic software package.[13]

Electrical Conductivity Measurements. The temperature dependence of the electrical resistivity was measured by the four-probe method using a constant current ranging from 10 to 100 mA. Gold wires (15 μm) were fixed on the surface along the long axis of the crystal by a gold paint. Measurements under pressure were performed up to 6 kbar for $[Me_3HN][Ni(dmise)_2]_2$ using a clamp-type cell and Daphne oil 7373 (Idemitsu Oil Co. Ltd.) as the pressure medium.

Band Structure Calculation. Band structure calculations were carried out on $[Me_3HN][Ni(dmise)_2]_2$ and $[Me_2H_2N][Ni(dmise)_2]_2$ by the extended Hückel method by using Slater-type atomic orbitals. The exponents ζ and ionization potentials (eV) for atomic orbitals are listed in Table 2.

Results and Discussions

Crystal Structures of $[Me_xH_{4-x}N][Ni(dmise)_2]_2$ ($x = 1-3$). The atomic coordinates of $[Me_3HN][Ni(dmise)_2]_2$ and $[Me_2H_2N][Ni(dmise)_2]_2$ are listed in Table 3a,b. The crystals belong to the triclinic system with space group $P\bar{1}$. The crystal structures of $[Me_3HN][Ni(dmise)_2]_2$ and $[Me_2H_2N][Ni(dmise)_2]_2$ are shown in Figure 2a,b. $Ni(dmise)_2$ sheets and the cation sheets arranged alternately along the *b* direction. Although the unit cell parameters are very similar to each other (see Table 1), $[Me_3HN][Ni(dmise)_2]_2$ and $[Me_2H_2N][Ni(dmise)_2]_2$ are not isostructural. $[Me_3HN][Ni(dmise)_2]_2$ is isostructural to $[Me_3HN][Ni(dmit)_2]_2$, while $[Me_2H_2N][Ni(dmise)_2]_2$ is isostruc-

(12) *International Tables for X-ray Crystallography*; Kynoch Press: Birmingham, 1974; Vol. 4.
(13) Crystal Structure Analysis Package, Molecular Structure Corporation, 1985 and 1992.
(14) Sakurai, T.; Kobayashi, K. *Rep. Inst. Phys. Chem. Res.* **1979**, *55*, 69.

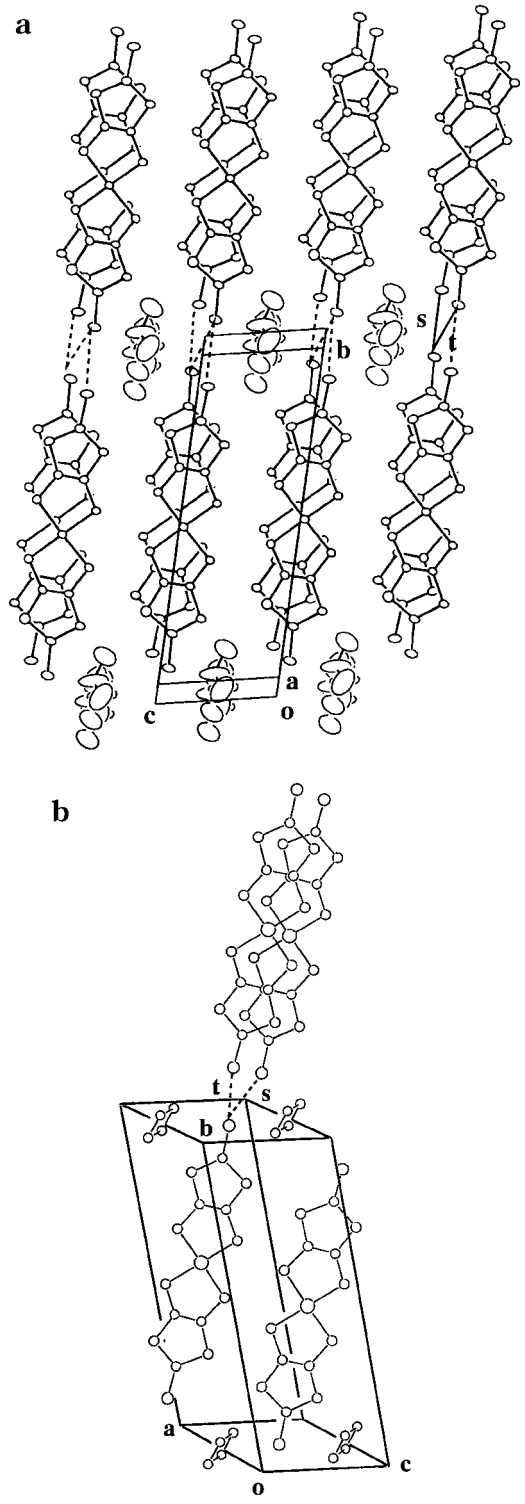

Figure 2. Crystal structures of (a) $[Me_3HN][Ni(dmise)_2]_2$ and (b) $[Me_2H_2N][Ni(dmise)_2]_2$. *s* and *t* correspond to discussions of the intermolecular chalcogen···chalcogen distances and the overlap integrals. Me_3HN^+ and $Me_2H_2N^+$ cations are disordered.

tural to $[Me_2H_2N][Ni(dmit)_2]_2$.[15] Each unit cell contained two $Ni(dmise)_2$ molecules and one countercation. Selected bond lengths and angles are listed in Table 4a,b. In $[Me_3HN][Ni(dmise)_2]_2$, the $Ni(dmise)_2$ molecules stack along the [100] with slightly dimerized stacks (3.557 and 3.464 Å), and in $[Me_2H_2N][Ni(dmise)_2]_2$, along the [101] with spacings 3.573 and 3.522 Å, respectively (Figure 3a,b). In each case, the $Ni(dmise)_2$ molecules formed one-dimensional columns. In $[Me_3HN][Ni(dmise)_2]_2$ and $[Me_2H_2N][Ni(dmise)_2]_2$, the cations are located on the inversion center, so that the cations have positional disorder and the carbon and nitrogen atoms have large thermal parameters. Intermolecular contacts between the chalcogen atoms at less than the sum of the van der Waals radii (S···S, 3.70 Å; S···Se, 3.85 Å; Se···Se, 4.0 Å) of $[Me_3HN][Ni(dmise)_2]_2$ and $[Me_2H_2N][Ni(dmise)_2]_2$ are listed in Table 5. The short intermolecular contacts of the chalcogen··· chalcogen atoms were observed along the stacking direction of $Ni(dmise)_2$ molecules, the transverse direction and along the long axis of the molecule. The Se···Se short contacts along the long axis of the molecules are 3.801(1) and 3.486(1) Å in

Table 4. Selected Bond Lengths (Å) and Angles (deg) for $[Me_3HN][Ni(dmise)_2]_2$ and $[Me_2H_2N][Ni(dmise)_2]_2$

(a) $[Me_3HN][Ni(dmise)_2]_2$

Ni−S1	2.151(2)	S7−C4	1.730(5)
Ni−S2	2.167(2)	S7−C6	1.714(5)
Ni−S5	2.155(2)	S8−C5	1.738(5)
Ni−S6	2.168(2)	S8−C6	1.741(5)
S1−C1	1.686(5)	Se1−C3	1.788(5)
S2−C2	1.693(5)	Se2−C6	1.782(5)
S3−C1	1.737(5)	C1−C2	1.372(6)
S3−C3	1.710(5)	C4−C5	1.374(6)
S4−C2	1.747(5)	N−C7	1.38(1)
S4−C3	1.731(5)	N−C8	1.36(1)
S5−C4	1.696(5)		
S6−C5	1.710(5)		
S1−Ni−S2	92.86(6)	S5−C4−C5	121.4(4)
S5−Ni−S6	93.66(6)	S7−C4−C5	115.8(4)
Ni−S1−C1	102.6(2)	S6−C5−C4	121.5(4)
Ni−S2−C2	101.8(2)	S8−C5−C4	115.2(4)
Ni−S5−C4	102.1(2)	S7−C6−S9	112.2(3)
Ni−S6−C5	101.3(2)	S7−C6−Se2	123.4(3)
S1−C1−C2	121.2(4)	S8−C6−Se2	124.4(3)
S3−C1−C2	116.3(4)	C1−S3−C3	97.6(2)
S2−C2−C1	121.5(4)	C2−S4−C3	97.4(2)
S4−C2−C1	115.0(4)	C4−S7−C6	98.7(2)
S3−C3−S4	113.6(3)	C5−S8−C6	98.0(2)
S3−C3−Se1	122.1(3)	C7−N−C8	67.7(4)
S4−C3−Se1	124.3(3)		

(b) $[Me_2H_2N][Ni(dmise)_2]_2$

Ni−S1	2.165(4)	S7−C3	1.732(1)
Ni−S2	2.160(5)	S7−C6	1.74(2)
Ni−S3	2.171(5)	S8−C4	1.73(1)
Ni−S4	2.154(4)	S8−C6	1.71(2)
S1−C1	1.71(2)	Se1−C5	1.79(1)
S2−C2	1.70(1)	Se2−C6	1.80(1)
S3−C3	1.70(1)	C1−C2	1.37(3)
S3−C4	1.70(2)	C3−C4	1.38(2)
S5−C1	1.74(1)	N−C11	1.14(5)
S5−C5	1.73(2)	N−C12	1.16(5)
S6−C2	1.75(2)		
S6−C5	1.73(2)		
S1−Ni−S2	93.3(2)	S7−C3−C4	115.3(10)
S3−Ni−S4	92.7(2)	S7−C6−S8	114.1(7)
Ni−S1−C1	102.1(6)	S8−C4−C3	116.2(10)
Ni−S2−C2	101.8(6)	Se1−C5−S5	123.6(9)
Ni−S3−C3	102.5(6)	Se1−C5−S6	123.1(10)
Ni−S4−C4	102.8(6)	Se2−C6−S7	124.0(10)
S1−C1−C2	121(1)	Se2−C6−S8	121.9(9)
S2−C2−C1	122(1)	C1−S5−C5	97.9(8)
S3−C3−C4	121(1)	C2−S6−C5	97.6(8)
S4−C4−C3	121.4(10)	C3−S7−C6	97.2(7)
S5−C5−S6	113.2(7)	C4−S8−C6	97.3(7)
S5−C1−C2	115.6(11)	C11−N−C12	161(4)
S6−C2−C1	115.7(10)		

(15) (a) Pomarede, B.; Garreau, B.; Malfant, I.; Valade, L.; Cassoux, P.; Legros, J. P.; Audouard, A.; Brossard, L.; Ulmet, J. P.; Doublet, M. L.; Canadel, E. *Inorg. Chem.* **1991**, *33*, 3401. (b) Ulmet, J. P.; Mazzaschi, M.; Tejel, C.; Cassoux, P.; Brossard, L. *Solid State Commun.* **1990**, *74*, 91. (c) Legros, J. P.; Valade, L.; Barreau, B.; Pomarede, B.; Cassoux, P.; Brossard, L.; Dybois, S.; Audouard, A; Ulmet, J. P. *Synth. Met. 1993*, 2146.

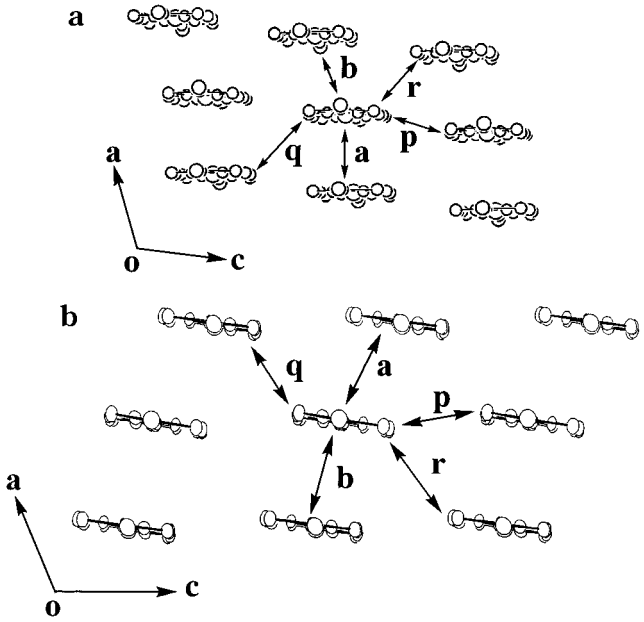

Figure 3. End-on prejections of (a) $[Me_3HN][Ni(dmise)_2]_2$ and (b) $[Me_2H_2N][Ni(dmise)_2]_2$. These figures indicate the schemes of intermolecular short contacts between chalcogen atoms less than the sum of the van der Waals radii and their overlap integrals.

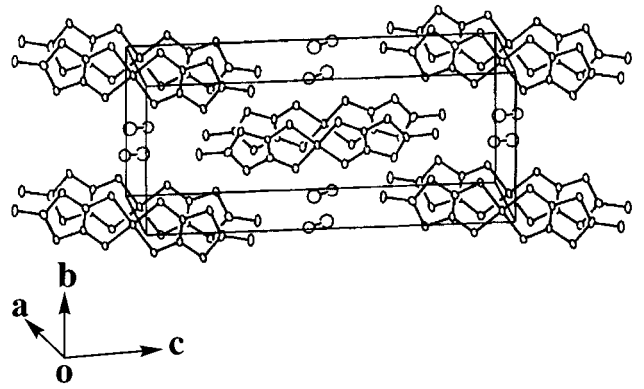

Figure 4. Crystal structure of $[MeH_3N][Ni(dmise)_2]_2$. MeH_3N^+ cations disorderedly occupy two sites.

$[Me_3HN][Ni(dmise)_2]_2$ and 3.504(3) and 3.617(3) Å in $[Me_2H_2N]$-$[Ni(dmise)_2]_2$, which are longer than the 3.277(3) Å contacts in α-$[Me_4N][Ni(dmise)_2]_2$. $[Me_3HN][Ni(dmise)_2]_2$ and $[Me_2H_2N]$-$[Ni(dmise)_2]_2$ have large values of intermolecular overlap integrals along the long axis of the molecules, which is quite different from the case of α-$[Me_4N][Ni(dmise)_2]_2$.[3] The results of band structure calculation are discussed later.

At first $[MeH_3N][Ni(dmise)_2]_2$ having a smaller countercation was expected to give larger overlap integrals between the selone groups. However, unexpectedly, the crystal structure of $[MeH_3N][Ni(dmise)_2]_2$ was different from those of $[Me_3HN]$-$[Ni(dmise)_2]_2$ and $[Me_2H_2N][Ni(dmise)_2]_2$. The crystal belongs to the monoclinic system with the space group $P2_1/c$. The structure is shown in Figure 1c. Atomic coordinates of $[MeH_3N][Ni(dmise)_2]_2$ are listed in Table 6. Selected bond lengths and angles are listed in Table 7. The crystal structure of $[MeH_3N][Ni(dmise)_2]_2$ is shown in Figure 4. The $Ni(dmise)_2$ molecules and MeH_3N^+ cations arrange alternately in the [100] plane. There were no short intermolecular interactions between selone groups of the $Ni(dmise)_2$ molecules (Table 8). The MeH_3N^+ cation located near the inversion center took two possible orientations. The $Ni(dmise)_2$ molecules stack with spacings 3.608 and 3.602 Å along the [100] direction (Figure 5).

Table 5. Intermolecular Chalcogen···Chalcogen Distances in $[Me_3HN][Ni(dmise)_2]_2$ and $[Me_2H_2N][Ni(dmise)_2]_2$[a]

	contact	symmetry operation[b]	distance, (Å)
		(a) $[Me_3HN][Ni(dmise)_2]_2$	
a	S1···S2	$(-x, -y+1, -z)$	3.606(2)
	S1···S6	$(-x, -y+1, -z)$	3.677(2)
b	Se1···Se2	$(-x+1, -y+1, -z)$	3.773(2)
p	S1···S6	$(x, y, z+1)$	3.690(2)
r	S1···S1	$(-x+1, -y+1, -z+1)$	3.568(3)
	S1···S5	$(-x+1, -y+1, -z+1)$	3.661(2)
	S3···S5	$(-x+1, -y+1, -z+1)$	3.516(2)
	S3···S7	$(-x+1, -y+1, -z+1)$	3.653(2)
s	Se1···Se2	$(x, y-1, z)$	3.8007(9)
t	Se2···Se2	$(-x+1, -y+2, -z)$	3.486(1)
		(b) $[Me_2H_2N][Ni(dmise)_2]_2$	
a	S4···S4	$(-x+2, -y+1, -z)$	3.536(7)
	S2···S4	$(-x+2, -y+1, -z)$	3.647(6)
	S2···S8	$(-x+2, -y+1, -z)$	3.510(6)
b	S1···S8	$(-x+1, -y+1, -z)$	3.664(5)
p	S1···S2	$(x, y, z+1)$	3.600(5)
	S1···S4	$(x, y, z+1)$	3.564(6)
	S3···S4	$(x, y, z+1)$	3.633(5)
	S3···S8	$(x, y, z+1)$	3.615(5)
q	Se1···Se2	$(-x+2, -y+1, -z+1)$	3.831(3)
s	Se1···Se1	$(-x+2, -y+2, -z+2)$	3.504(3)
t	Se1···Se2	$(x, y+1, z+1)$	3.617(3)

[a] *a*, *b*, *p*, *q*, *r*, *s*, and *t* correspond to Figure 3. [b] This applies on the second atom.

Table 6. Atomic Coordinates of $[MeH_3N][Ni(dmise)_2]_2$

atom	*x*	*y*	*z*	B_{eq}[a]
Se1	0.0973(2)	0.9148(2)	0.28915(6)	4.45(4)
Se2	0.4266(2)	1.0840(2)	−0.33389(6)	4.82(4)
Ni	0.2612(2)	1.0059(2)	−0.02214(7)	2.95(3)
S1	0.2831(5)	1.1433(3)	0.0539(1)	3.41(8)
S2	0.1748(5)	0.8335(4)	0.0302(1)	3.94(9)
S3	0.3458(4)	1.1789(4)	−0.0757(1)	3.41(8)
S4	0.2387(5)	0.8641(4)	−0.0967(1)	3.41(8)
S5	0.2091(4)	1.0939(4)	0.1835(1)	3.47(8)
S6	0.1065(5)	0.8062(4)	0.1600(1)	3.51(8)
S7	0.4070(5)	1.1965(4)	−0.2064(1)	3.45(8)
S8	0.3067(4)	0.9091(4)	−0.2270(1)	3.19(8)
N	0.184(4)	1.000(3)	0.500(1)	8.8(8)
C1	0.219(1)	1.039(1)	0.1104(5)	2.8(3)
C2	0.171(1)	0.901(1)	0.998(5)	2.7(3)
C3	0.347(1)	1.102(1)	−0.1449(5)	2.9(3)
C4	0.302(2)	0.967(1)	−0.1541(5)	2.6(3)
C5	0.138(1)	0.940(1)	0.940(1)	3.0(3)
C6	0.380(2)	1.062(1)	−0.2577(5)	3.5(3)
C8	0.104(5)	0.985(4)	0.447(2)	6.4(10)

[a] $B_{eq} = (8/3)\pi^2(U_{11}(aa^*)^2 + U_{22}(bb^*)^2 + U_{33}(cc^*)^2 + 2U_{12}aa^*bb^* \cos\gamma + 2U_{13}aa^*cc^* \cos\beta + 2U_{23}cc^*bb^* \cos\alpha)$.

The Electrical Conductivity of $[Me_xH_{4-x}N][Ni(dmise)_2]_2$ ($x = 1-3$). Figure 6 shows the temperature dependence of the electrical resistivity of $[Me_3HN][Ni(dmise)_2]_2$. The conductivity is 100 S cm^{-1} around room temperature and exhibited weakly metallic behavior around room temperature at ambient pressure. In the low-temperature region, the resistivity gradually increased. The activation energy below 25 K was 0.055 eV. Such behavior is similar to that of $[Me_3HN][Ni(dmit)_2]_2$.[15] However, the electrical resistivity of $[Me_3HN][Ni(dmit)_2]_2$ indicated sample dependencies, but that of $[Me_3HN][Ni(dmise)_2]_2$ did not. Under high pressures, the metallic range extended down to ca. 150 K at 3 kbar and down to ca. 60 K at 6 kbar, respectively. The increase of resistivity at low temperature was not suppressed by applying pressure. Although the crystal quality of the samples was not sufficient, all of the crystals measured showed almost identical resistivity behavior. Similar weakly metallic temperature dependences of the resistivities have been frequently observed in $M(dmit)_2$ conductors.

Table 7. Selected Bond Lengths (Å) and Angles (deg) for $[MeH_3N][Ni(dmise)_2]_2$

Ni−S1	2.160(5)	S7−C3	1.74(2)
Ni−S2	2.150(5)	S7−C6	1.73(2)
Ni−S3	2.165(5)	S8−C4	1.74(1)
Ni−S4	2.162(5)	S8−C6	1.71(2)
S1−C1	1.71(2)	Se1−C5	1.79(1)
S2−C2	1.69(1)	Se2−C6	1.79(2)
S3−C3	1.72(2)	C1−C2	1.39(2)
S4−C4	1.71(5)	C4−C5	1.35(2)
S5−C1	1.73(1)	N−C8	1.35(2)
S5−C5	1.70(2)		
S6−C2	1.73(1)		
S6−C5	1.76(2)		
S1−Ni−S2	92.3(2)	S4−C4−C3	120(1)
S3−Ni−S4	93.3(2)	S8−C4−C3	115(1)
Ni−S1−C1	103.1(5)	S5−C5−C6	113.8(8)
Ni−S2−C2	103.1(5)	S5−C5−Se1	124.6(10)
Ni−S3−C3	101.1(6)	S6−C5−Se1	121.6(9)
Ni−S4−C4	102.3(5)	S7−C6−S8	113.4(9)
S1−C1−C2	120(1)	S8−C6−Se2	122.0(9)
S5−C1−C2	115(1)	S8−C6−Se2	124.6(9)
S2−C2−C1	120(1)	C1−S5−C3	98.1(7)
S6−C2−C1	115(1)	C2−S6−C5	98.7(7)
S3−C3−C4	122(1)	C5−S7−C6	96.7(8)
s7−C3−C4	116(1)	C4−S8−C6	97.8(7)

Table 8. Intermolecular Chalcogen···Chalcogen Distances in $[MeH_3N][Ni(dmise)_2]_2$[a]

	contact	symmetry operation[b]	distance, (Å)
a	Se1···Se2	$(-x+1, -y+2, -z)$	3.723(3)
b	Se1···S8	$(-x, -y+2, -z)$	3.722(5)
q	S7···S8	$(-x+1, y+1/2, -z-1/2)$	3.386(6)
r	Se2···S1	$(-x, -y+2^1/_2, -z-1/2)$	3.755(5)
	Se2···S5	$(-x, -y+2^1/_2, -z-1/2)$	3.529(5)
	S5···S7	$(-x, -y+2^1/_2, z+1/2)$	3.476(6)
s	Se1···S8	$(x, -y-1^1/_2, z+1/2)$	3.511(5)
	Se1···S4	$(x, -y+1^1/_2, z+1/2)$	3.817(5)
	S6···S8	$(x, -y+1^1/_2, z+1/2)$	3.560(6)

[a] *a*, *b*, *q*, *r*, and *s* correspond to Figure 5. [b] This applies on the second atom.

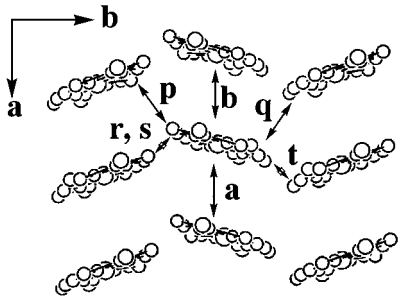

Figure 5. End-on projection of $[MeH_3N][Ni(dmise)_2]_2$. This figure indicates the short intermolecular contacts between chalcogen atoms less than the sum of the van der Waals radii and their overlap integrals.

Figure 7 shows the temperature dependence of the resistivity of $[Me_2H_2N][Ni(dmise)_2]_2$. The electrical conductivity of $[Me_2H_2N][Ni(dmise)_2]_2$ was ca. 30 S cm^{-1} around room temperature. The resistivity was almost constant around room temperature and increased below 100 K. (The activation energy was 0.04 eV in the range 54.3−61.3 K.) In addition to the inferior quality of the crystal, the crystal was observed to be unstable in the air, which could have something to do with the sluggish temperature dependence of the resistivity.

The conductivity of $[MeH_3N][Ni(dmise)_2]_2$ is 4.5 S cm^{-1} around room temperature. The temperature dependence of electrical resistvity is semiconductive in the whole temperature range (Figure 8). The activation energy was 0.072 eV.

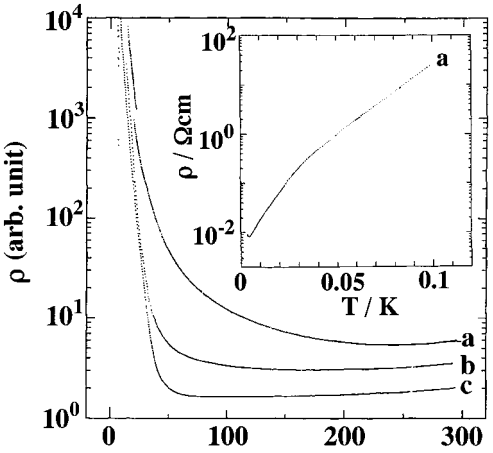

Figure 6. Temperature dependence of electrical resistivities of $[Me_3HN][Ni(dmise)_2]_2$: (a) at ambient pressure, (b) at 3 kbar, and (c) at 6 kbar. The conductivity was about 100 S cm^{-1} at room temperature and ambient pressure. The activation energy below 25 K was 0.055 eV.

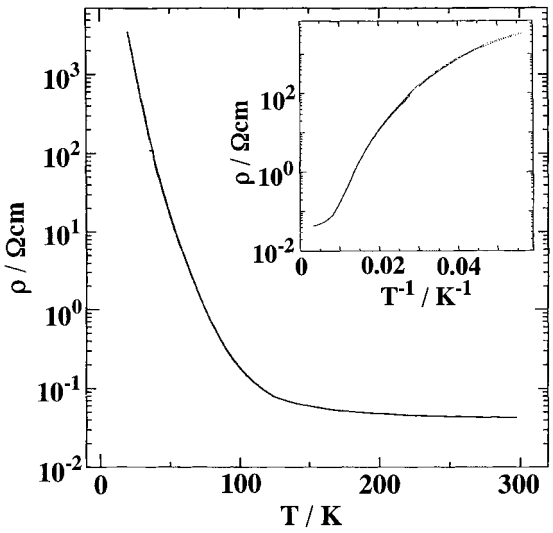

Figure 7. Temperature dependence of electrical resistivity of $[Me_2H_2N][Ni(dmise)_2]_2$ at ambient pressure. The conductivity was about 30 S cm^{-1} at room temperature. The activation energy in the range 54−61 K was 0.04 eV.

Band Structures of $[Me_3HN][Ni(dmise)_2]_2$ and $[Me_2H_2N][Ni(dmise)_2]_2$. Tight-binding band structure calculations were performed by the simple extended Hückel method using the LUMO of $Ni(dmise)_2$.[16,17] The overlap integrals are tabulated in Table 9. Since $|a|$ and $|b|$ take similar values, the $Ni(dmise)_2$ stack can be regarded as regular from the viewpoint of electronic band structure. This is consistent with the idea that the conduction band is formed from the LUMO. The overlap integrals q in $[Me_3HN][Ni(dmise)_2]_2$ and r in $[Me_2H_2N][Ni(dmise)_2]_2$ have large values. This suggests that these salts have stronger transverse interactions compared with those of $M(dmit)_2$ compounds having similar arrangements. In addition, the overlap integrals of the molecules across the cation layer have fairly large values ($(2.0-3.0) \times 10^{-3}$) in $[Me_3HN][Ni(dmise)_2]_2$ and $[Me_2H_2N][Ni(dmise)_2]_2$. This is in striking contrast to the

(16) The main aim of our band structure calculations of the $Ni(dmise)_2$ compounds is to know the dimensionality of the band structure. The three-dimensionality of the band structures elucidated by the present band calculations will not be affected by the inclusion of HOMO orbitals, as the dimeric nature of $[Me_3HN][Ni(dmise)_2]_2$ and $[Me_2H_2N][Ni(dmise)_2]_2$ is very weak, comparable to that of $Me_4N[Ni(dmit)_2]_2$.[17]

(17) Canadell, E.; Ravy, S.; Pouget J. P. *Solid State Commun.* **1990**, *75*, 633.

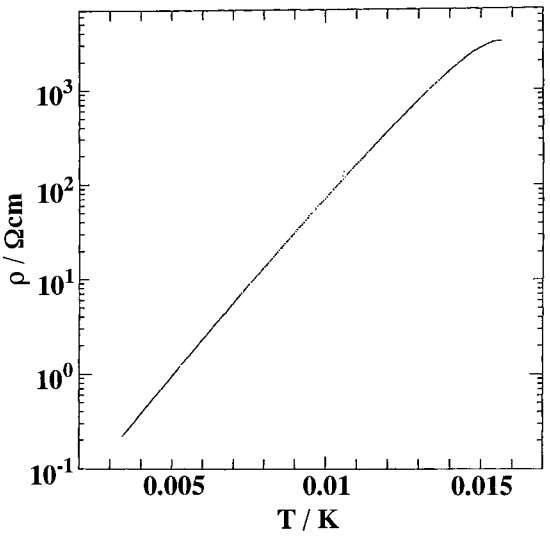

Figure 8. Temperature dependence of electrical resistivity of $[MeH_3N][Ni(dmise)_2]_2$. The conductivity was about 4.5 S cm^{-1} at room temperature and ambient pressure. The activation energy was 0.072 eV.

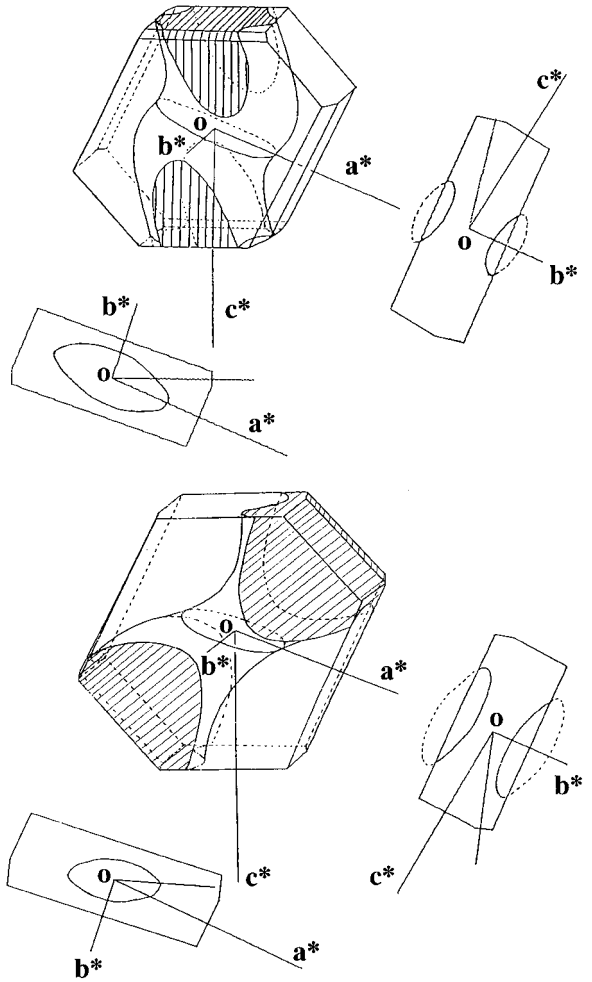

Figure 9. Calculated Fermi surfaces of (a, top) $[Me_3HN][Ni(dmise)_2]_2$ and (b, bottom) $[Me_2H_2N][Ni(dmise)_2]_2$.

case of α-$[Me_4N][Ni(dmise)_2]_2$,which has small overlap integrals along the direction of the long axis of the molecule.[3]

Figure 9 shows the calculated Fermi surfaces of the two compounds. The cross sections of Fermi surfaces in the a^*b^* and b^*c^* planes showed closed Fermi surfaces. Since the Fermi surfaces gave closed cross sections in two different directions, these two $Ni(dmise)_2$ conductors can be regarded as essentially

Table 9. Intermolecular Overlap Integrals ($\times 10^3$) of $Ni(dmise)_2$ in $[Me_3HN][Ni(dmise)_2]_2$, $[Me_2H_2N][Ni(dmise)_2]_2$, and $[MeH_3N][Ni(dmise)_2]_2$[a]

		(a) $[Me_3HN][Ni(dmise)_2]_2$			
a	12.7	*p*	0.2	*s*	3.0
b	−14.0	*q*	−4.9	*t*	0.7
		r	1.3		
		(b) $[Me_2H_2N][Ni(dmise)_2]_2$			
a	−14.9	*p*	0.2	*s*	2.0
b	13.4	*q*	1.3	*t*	2.9
		r	−6.5		
		(c) $[MeH_3N][Ni(dmise)_2]_2$			
a	−21.4	*p*	0.25	*r*	0.24
b	7.11	*q*	0.25	*s*	0.24
				t	0.34

[a] *a*, *b*, *p*, *q*, *r*, *s*, and *t* in sections a and b and in section c correspond to Figures 3 and 5, respectively.

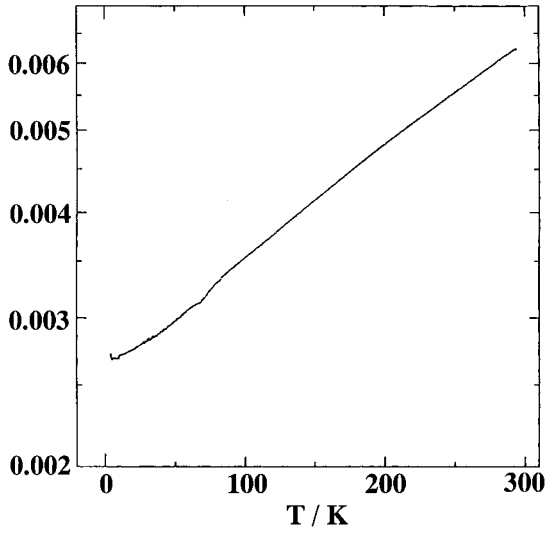

Figure 10. Temperature dependence of electrical resistivity of $Cs[Pd(dmise)_2]_2$.

three-dimensional conductors. The weak metallic nature of these systems should be related to the relatively small overlap integrals (transfer integrals) of LUMOs. The low crystal quality and the positional disorder in the cation layers are also undesirable for the enhancement of the metallic nature of the system. In addition, the low-temperature semiconductive properties are considered to be of an intrinsic nature for these $Ni(dmise)_2$ salts. However, the result of the band structure calculations clearly shows a way to design a stable three-dimensional molecular metal for planar π molecules.

The Electrical Conductivity of $Cs[Pd(dmise)_2]_2$. The poor quality of the crystal prevented a complete crystal structure determination. The X-ray photographs showed that one of the lattice constants was about 4 Å. Weak diffuse spots were also observed among clear Bragg spots. This lattice constant suggests that it is not isostructural to $Cs[Pd(dmit)_2]_2$ ($Cs[Pd(dmit)_2]_2$: monoclinic, $C2/c$, $a = 14.490(4)$ Å, $b = 6.2629(14)$, $c = 30.601(7)$, $\beta = 90.58(2)°$, $V = 2777.02$ Å^3, $Z = 4$).[18] The resistivity decreased slowly with decreasing temperature down to 4.2 K. The weak temperature dependence should be related to the poor quality of the crystals (see Figure 10).

$Cs[Pd(dmise)_2]_2$ is the first example of a $M(dmise)_2$ compound which has metallic conductivity down to 4 K. Attempts

(18) Underhill, A. E.; Clark, R. A.; Marsden, I.; Allan, M.; Friend, R. H.; Tajima, H.; Naito, T.; Tamura, M.; Kuroda, H.; Kobayashi, A.; Kobayashi, H.; Canadell, E.; Ravy, S.; Pouget, J. P. *J. Phys.: Condens. Matter* **1991**, *3*, 933.

to prepare single crystals of sodium or potassium salts were not successful. However, considering the fact that, even in the $M(dmit)_2$ conductors extensively studied so far, there are only a few systems having a stable metallic state down to low temperature, the stable metallic state of $Cs[Pd(dmise)_2]_2$ is noteworthy. In the case of $M(dmit)_2$ conductors, all of the compounds with a stable metallic state have characteristic molecular arrangements called "spanning overlap mode". But the lattice constant of 4 Å of the Cs salt indicates that $M(dmise)_2$ conductors can have stable metallic states even in different molecular arrangements. Although the dimensionality of the metallic state of $Cs[Pd(dmise)_2]_2$ could not be examined due to the poor crystal quality, the stable metallic state suggests a two- or three-dimensional nature of the system. The small size of the Cs^+ ions, as compared with $(CH_3)_xH_{4-x}N^+$ ions, indicates that selone···selone contacts will be much closer. If we can obtain a good single crystal of (alkali metal)$[M(dmise)_2]_2$, there may be a possibility that a stable molecular metal system with a three-dimensional Fermi surface at low temperature will result.

Conclusion

New radical salts of $M(dmise)_2$ were synthesized, and their electrical conductivities were studied. Among them, $Cs[Pd(dmise)_2]_2$ retained metallic behavior down to 4 K at ambient pressure. $[Me_3HN][Ni(dmise)_2]_2$ exhibited weak metallic behavior around room temperature. Tight-binding band structure calculations suggested that $[Me_3HN][Ni(dmise)_2]_2$ and $[Me_2H_2N][Ni(dmise)_2]_2$ have three-dimensional Fermi surfaces. The intermolecular interactions between the selenium atoms in the selone group should be very effective to extend the dimensionality of $M(dmise)_2$ systems.

Supporting Information Available: Three X-ray crystallographic files, in CIF format, are available. Access information is given on any current masthead page.

IC970507J